Branching Ratios for Dissociative Recombination of $^{15}N^{14}N^+$

D. Kella, P. J. Johnson, H. B. Pedersen, L. Vejby-Christensen, and L. H. Andersen
Institute of Physics and Astronomy, University of Aarhus, DK-8000 Aarhus C, Denmark
(Received 26 April 1996)

Branching ratios for dissociative recombination of $^{15}N^{14}N^+$ molecular ions in the $X\,^2\Sigma_g^+$ electronic ground state were measured by a molecular imaging technique at the heavy ion storage ring ASTRID. For $v = 0$, the branching ratios for the final channels [$N(^4S) + N(^2D)$:$N(^4S) + N(^2P)$:$N(^2D) + N(^2D)$] were found to be (0.46:0.08:0.46). The fact that the $N(^4S) + N(^2D)$ and $N(^2D) + N(^2D)$ channels dominate is in agreement with recent multichannel quantum-defect theory calculations. Implications for modeling of the Martian atmosphere are discussed. [S0031-9007(96)01250-1]

PACS numbers: 34.80.Ht, 32.70.Cs, 39.90.+9, 96.30.Gc

Dissociative recombination (DR) of a diatomic molecular ion can be described by the following equation (initial state → final state):

$$AB(n, v, J)^+ + e^- + \varepsilon \rightarrow A(\alpha) + B(\beta) + \mathrm{KER}, \quad (1)$$

where AB^+ is a molecular ion in some n-electronic, v-vibrational, and J-rotational level, ε is the kinetic energy of the incoming electron in the center-of-mass frame, $A(\alpha)$ and $B(\beta)$ are the resulting atoms in the α and β electronic states, respectively, and KER is the kinetic energy release. Thus, the DR process may provide atoms with kinetic energy as well as electronic excitation. By measuring the KER, one can obtain information about both the initial molecular state and the final atomic electronic states of the DR process [1]. In the present work, this has been used to measure the DR branching ratios of $^{15}N^{14}N^+$.

DR of N_2^+ is important for the understanding of molecular physics, plasmas, and the chemistry of planetary ionospheres. The nitrogen atoms may be formed in the ^4S, ^2D, or ^2P states. $N(^2D)$ atoms are a major source for the production of N^+ by charge exchange with O^+ above 250 km in the atmosphere of the Earth [2] and an important source of NO through the interaction with O_2 in the terrestrial atmosphere and with CO_2 in the atmospheres of Venus and Mars [3]. In the Martian atmosphere, the KER in the DR process may play an important role in the abnormal ^{15}N:^{14}N ratio due to the preferred escape of the lighter isotope [3]. Modeling of the atmospheres requires knowledge about the total DR cross section (measured, e.g., by Canosa *et al.* [4]) and the probability of reaching any of the available atomic limits from each of the initial vibrational levels (i.e., branching ratios).

Figure 1 displays the potential-energy curve (PEC) for the electronic ground state of N_2^+, $X\,^2\Sigma_g^+$, as well as the PEC for the first excited state $A\,^2\Pi_u$. We also show the N_2 repulsive states of $^3\Pi_u$ symmetry since this electronic symmetry has been identified as the most important symmetry for DR from the $v = 0$ ion level [5].

DR of $^{15}N^{14}N^+$ may produce N atoms in the following four channels (see Ref. [6] and Fig. 1):

$$N(^4S) + N(^2D) + 3.44\ \mathrm{eV} + E_{v,j}, \quad (a)$$

$$N(^4S) + N(^2P) + 2.24\ \mathrm{eV} + E_{v,j}, \quad (b)$$

$$N(^2D) + N(^2D) + 1.05\ \mathrm{eV} + E_{v,j}, \quad (c)$$

$$N(^2D) + N(^2P) - 0.14\ \mathrm{eV} + E_{v,j}, \quad (d)$$

where $E_{v,j}$ is the contribution from the initial ro-vibrational excitation energy to the KER (the vibrational separation is 2173.05 cm^{-1} and the rotational constant $B = 1.87\ \mathrm{cm}^{-1}$ [7]). A fifth channel, leading to the ground electronic limit [$N(^4S) + N(^4S)$], is not expected to play any role [5].

The theoretical understanding of the DR process requires detailed knowledge about (i) the PECs of the initial N_2^+ molecular ion and the repulsive curves of

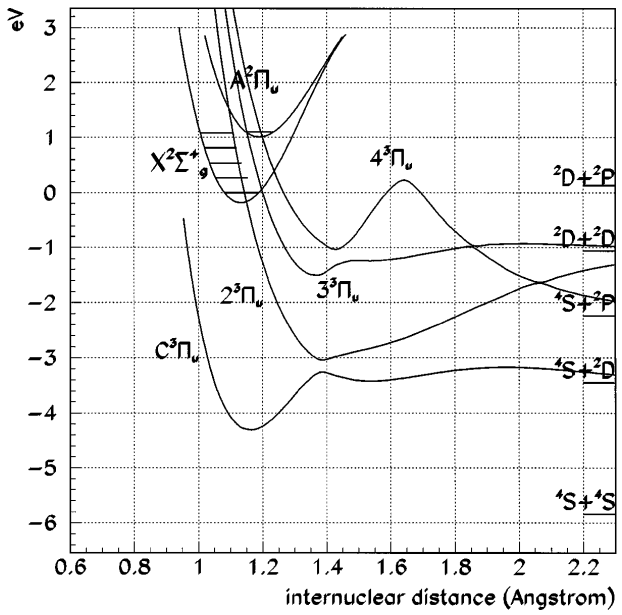

FIG. 1. A schematic representation of the lowest potential energy curves of the N_2^+ molecule together with the $^3\Pi_u$ neutral curves [8]. To the right are shown energy levels of the separated neutral atoms.

 0031-9007/96/77(12)/2432(4)$10.00

the doubly excited N_2 neutral molecule, (ii) the capture width of the relevant N_2 PECs, and (iii) the progression along the repulsive curves to the final atomic limits. Accurate values for the branching ratios provide a means to improving the understanding of the complicated transition from the initial molecular-ion state to the final atomic limits in the DR process. In the particular case of DR of N_2^+, there are several dissociative routes with the same electronic symmetry, the couplings of which strongly influence the dynamics of the DR process [8].

The present measurement was performed at ASTRID, the Aarhus Storage Ring Denmark [9]. To reduce the probability of CO^+ isobar contamination in the beam, and to allow some rovibrational relaxation by dipole-allowed radiative transitions, the experiment was performed with a $^{15}N^{14}N^+$ beam which was produced in a standard plasma ion source [10] from a mixture of $^{30}N_2$ and $^{28}N_2$. Thus, a range of rovibrational levels may be populated in the beam. The beam was injected into the ring with 150 keV kinetic energy and then, after acceleration to 4.21 MeV during 4 s, data were collected over a period of 12 s. During these 12 s, an electron beam was merged with the ion beam at zero average relative velocity ($\langle\varepsilon\rangle = 0$) in the electron cooler. The vacuum was approximately 4×10^{-11} Torr, the ion-beam current approximately 50 nA at the beginning of the measuring period, and the lifetime τ of the beam was 1.8 s.

The electron cooler can provide a magnetically confined, adiabatically expanded electron beam with laboratory energies in the range of 40–2000 eV. In the present experiment, we had a transverse temperature of about 20 meV ($T = 230$ K) and a longitudinal temperature of about 1 meV ($T = 12$ K) (see Refs. [11,12]).

In order to probe the final-state distribution of the DR process, we measured the kinetic energy release of the dissociating molecules, using an imaging detector which was a 77-mm-diameter double-stage microchannel plate (MCP) with a phosphor anode [13]. Each fragment, which hit the detector, created a spot of light on the phosphor. The distance between these spots is a two-dimensional projection of the distance between the fragments. Light from the phosphor screen was detected by a standard charge-coupled device (CCD) camera and a photomultiplier. The photomultiplier signal was used as a trigger for a fast 2 μs switch which lowered the voltage to the phosphor anode. The time difference between two fragments of the same molecule hitting the detector was a few nanoseconds. Thus, for sufficiently low beam rates, the fast switch ensured that only fragments originating from a single molecule created light spots on the anode. By keeping the neutral beam rate below 5 kHz, the probability of more than one event being registered in the same video frame was less than 1%. The images recorded by the CCD camera were transferred frame by frame to a special video-acquisition card [13] in the data-acquisition computer.

The distribution of measured distances may be understood as follows [1]: Consider a molecular ion AB^+ with nuclear masses m_1 and m_2 and kinetic energy E_0. Denoting the distance from the interaction point to the detector by L, and the angle between the internuclear axis and the beam direction by θ, the distance R measured on the detector is

$$R = R_{\max} \sin\theta\,, \tag{2}$$

where

$$R_{\max} = \sqrt{\frac{\mathrm{KER}}{E_0}}\,\frac{m_1 + m_2}{\sqrt{m_1 m_2}}\,L = cL\,. \tag{3}$$

Assuming that the interaction with zero-velocity electrons results in an isotropic distribution in θ [$f(\theta) = 1$], the distribution of distances [$g_L(R)$] for a given L is derived from

$$\begin{aligned} g_L(R)dR &= f(\theta)\sin\theta\, d\theta \\ &= \frac{R/R_{\max}}{R_{\max}\sqrt{1 - (R/R_{\max})^2}}\,dR \end{aligned} \tag{4}$$

for $R \in (0, R_{\max})$ and zero otherwise. The final distribution of distances between the two fragments is obtained by integration over the cooler length $\Delta L = 95$ cm to give

$$\begin{aligned} F_{\mathrm{KER}}(R) &= \frac{1}{\Delta L}\int_{L_1}^{L_2} g_L(R)\,dL \\ &= \frac{1}{c\Delta L}\left[\arctan\frac{K(L_2)}{R} - \arctan\frac{K(L_1)}{R}\right], \end{aligned} \tag{5}$$

where $L_1 = L_0 - \Delta L/2$, $L_2 = L_0 + \Delta L/2$, $K(L_i) = \mathrm{Re}[\sqrt{(cL_i)^2 - R^2}]$, and $L_0 = 613$ cm was the distance from the center of the cooler to the imaging detector. Equation (5) describes the distribution corresponding to a single value of the kinetic energy release.

The results from the imaging experiment are shown in Fig. 2 which is a plot of the distribution of measured projected distances between fragments. The figure displays the data after background subtraction and a fit to the data which is explained below. The fifth, energetically allowed channel [$N(^4S) + N(^4S)$], which would produce a KER of 5.82 eV for $v = 0$, is not detected in our experiment since there is no statistically significant signal at distances above 13.5 mm. The $N(^2D) + N(^2P)$ channel is irrelevant for the rovibrational ground-state ions but energetically allowed for $v \geq 1$ and for ($v = 0, j > 24$). The transition from $v = 1, j = 0$ to the $N(^2D) + N(^2P)$ limit releases kinetic energy of only 0.13 eV. This energy may, however, be substantially larger when rotational excitation is taken into account. The jagged dash-dotted curve in the 1–4 mm region of Fig. 2 shows the expected contributions of the $v = 1$ and $v = 2$ levels to the $N(^2D) + N(^2P)$ channel when no rotational excitation is considered [Eq. (5)].

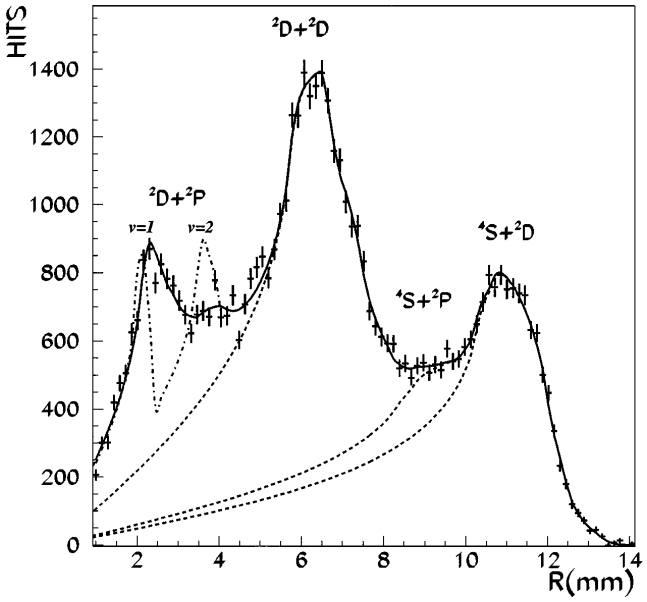

FIG. 2. The distribution of two-dimensional projected distances (R) between two nitrogen atoms (after background subtraction) and the curve depicting the model function with fitted $P(v, f)$ are shown. The region under the fit is divided by dashed lines to show the contributions to the four final electronic limits. On the left hand side ($R = 1-4$ mm) the dash-dotted line represents an attempt to describe the data without including rotational excitation.

To account for the wider features of the data in the 1–4 mm region, rotational excitation was taken into account. A general expression for the distribution of the distances is

$$D(R) = \text{const} \times \sum_{v,J,f} p(v, J) \langle \sigma_{v,J,f}(\text{v})\text{v} \rangle F_{\text{KER}}(R) , \tag{6}$$

where $p(v, J)$ is the population of the (v, J) rovibrational level in the molecular ion beam, $\sigma_{v,J,f}(\text{v})$ is the DR cross section which depends on the rovibrational level and the final channel $f = (a), \ldots, (d)$, v is the electron velocity in the molecular frame, and the brackets indicate a folding with the electron velocity distribution. $F_{\text{KER}}(R)$ is given in Eq. (5). Since the rotational dependence of the DR cross section is unknown, we assume that the cross section has a negligible rotational dependence. Further, we assume that the rotational population in the molecular beam is independent of v and is given by a Boltzmann distribution. Hence we obtain

$$D(R) = \sum_j (2j + 1) e^{-j(j+1)B/kT} \times \sum_v \sum_{f=(a)}^{(d)} P(v, f) F_{\text{KER}}(R) , \tag{7}$$

where kT is the rotational temperature and $P(v, f) = \text{const} \times p(v) \langle \sigma_{v,J,f}(\text{v})\text{v} \rangle$ the fit parameters which for each v yield the branching ratios. The data in Fig. 2 were fitted with the function $D(R)$ from Eq. (7) using $P(v, f)$ and kT as fit parameters. We included four vibrational levels ($v = 0-3$) and rotational levels up to $J = 60$.

The data show no measurable contributions from $v > 3$ levels. This fact is interesting in itself. A calculation, which takes into account only dipole-allowed transitions within the vibrational and rotational levels of the ground electronic state, shows that the lifetimes of the vibrational levels are from 10 s for the $v = 5$ level to 46 s for $v = 1$ [14,15]. Assuming that the various DR cross sections are not of different orders of magnitude, all these levels should contribute significantly during the measuring period from 4 to 16 s after injection. This vibrational cutoff may be explained by the proximity of the $A\,^2\Pi_u$ electronic state, for which the $v = 0$ level is just above $v = 4$ of the $X\,^2\Sigma_g^+$ ground electronic state (see Fig. 1 and Ref. [6]).

If we denote the branching ratios for each vibrational level by $b_a{:}b_b{:}b_c{:}b_d$, then, for $v = 0$, the fit yields

$$(b_a{:}b_b{:}b_c{:}b_d) = (0.46 \pm 0.06{:}0.08 \pm 0.06{:}0.46 \pm 0.06{:}0)$$

and for $v = 1$

$$(b_c{:}b_d) = (1 \pm 0.2{:}1 \pm 0.2) .$$

With the present experimental resolution, we were not able to obtain the branching ratios for higher vibrational levels and for the (a) and (b) channels for $v = 1$. Moreover, branching ratios for different vibrational levels could not be compared due to the lack of knowledge about the vibrational distribution in the beam. The temperature parameter resulting from the fit is $kT = 0.14$ eV, which is reasonable for the type of source used. The quoted uncertainties are extracted from the fit, considering the uncertainty of the length calibration and a variation of the temperature parameter. At the fitted temperature, rotationally excited ions of the $v = 0$ level could contribute to the spectrum below 2 mm via the (d) channel; however, no statistically significant contribution was found.

The present work was performed with $^{15}N^{14}N^+$. The small energy difference of about 2 meV between the ground-vibrational level of $^{15}N^{14}N^+$ and $^{28}N_2{}^+$ may, however, justify that we compare our results with a measurement [16] and calculations [5,8,17] performed with the homonuclear $^{28}N_2{}^+$.

Queffelec *et al.* measured the yield of $N(^2D)$ from the DR of $N_2{}^+$ in a flowing-afterglow device [16]. They found that the average yield was higher than 1.85, indicating that the major channel is the (c) channel ($b_c > 0.85$ and $b_a < 0.15$) [18]. It was argued that their $N_2{}^+$ population consisted mainly of ground-vibrational level ions caused by a resonant charge-exchange reaction. When coupled with the assumption of a ground-vibrational level population, their finding is inconsistent with our results [our $N(^2D)$ yield is 1.38 ± 0.13 for $v = 0$]. They further claimed that most atoms produced in a ^2P state would be

quenched to the ^2D state [19]. Assuming 100% quenching, our $v = 0$ results give a N(^2D) yield of 1.46 ± 0.15, which is still inconsistent with their results.

Guberman has performed a multichannel quantum-defect theory (MQDT) calculation based on the PECs shown in Fig. 1. One PEC ($2\,^2\Pi_u$) crosses the $v = 0$ level of the $X\,^2\Sigma_g^+$ ground state of N_2^+, and this curve is particularly important when low-energy electrons are considered. Guberman found that the dissociation following the initial capture from $v = 0$ leads almost exclusively to the (a) and (c) limits. This is in good agreement with our experiment where $b_a + b_c = 92\%$. We find that (a) and (c) channels have equal branching ratios. The calculation [5], which neglected the coupling between the $2\,^2\Pi_u$ and $4\,^2\Pi_u$ repulsive routes via Rydberg states and treated the avoided crossings at 1.3 and 1.9 Å (Fig. 1) by a Landau-Zener approximation, yielded $b_a = 88\%$ and $b_c = 12\%$. In a more recent preliminary calculation [17], Guberman obtained $b_a = 70\%$, $b_c = 27\%$, and $b_b = 3\%$ in better agreement with the experimental values.

One of the major questions asked about the DR process of the N_2^+ molecular ion is the following: What fraction of the molecules originally in the ground vibrational level ends up in the (a) limit? This question is relevant to the modeling of the evolution of the Martian atmosphere [3]. The Viking landers [20] measured the ^{15}N:^{14}N ratio in the Martian atmosphere to be 0.0060, which is 1.62 times the terrestrial value. The energy needed for the escape of a ^{14}N from the Martian exobase is 1.74 eV, while the limit for the heavier isotope is 1.86 eV. DR of $^{15}N^{14}N^+$ from the ground-vibrational level to the final (a) limit will result in a ^{14}N with 1.78 eV kinetic energy, while the heavier isotope would not have enough energy to escape. Thus a biasing effect is introduced via the DR process which preferably "ejects" ^{14}N from the upper Martian atmosphere.

Wallis calculated the probability of escape for ^{14}N and ^{15}N from the Martian exobase due to DR of $^{15}N^{14}N^+$ to the (a) limit, including the electron temperature [21]. He found that the major contribution to this biasing effect comes from the DR of $^{15}N^{14}N^+$ which originated from the ground-vibrational level and ended in the (a) limit. Furthermore, it was found that the effect nearly vanishes when the original vibrational level is higher. Fox [3] has shown that combining Wallis's and Guberman's calculations into the Martian atmosphere model leads to a higher ^{15}N:^{14}N ratio on Mars than measured. According to Fox, the lower ratio which was measured could be explained by assuming the existence of an early, dense atmosphere which damped the escape process. In view of our branching-ratio results the demand to use such an assumption in the modeling of the Martian atmosphere is weaker.

In conclusion, an imaging method was used to resolve not only the atomic limits but also vibrational and rotational features of the DR process with $^{15}N^{14}N^+$. We obtained branching ratios for the ground and first excited vibrational levels and made a direct observation of the opening of the N(^2D) + N(^2P) channel from the $v = 1$ level. The experiment as well as the MQDT calculation by Guberman show that the N(^4S) + N(^2D) and the N(^2D) + N(^2D) channels are dominant. In the experiment, the channels are of equal importance, whereas theory predicts a larger N(^4S) + N(^2D) yield.

We thank Oded Heber and Daniel Zajfman for the use of their MCP, Lorne Levinson for the modification of the "FTS" video acquisition card, and Jane Fox and Steven L. Guberman for helpful discussions. This project was supported by the Danish National Research Foundation through the Aarhus Center for Advanced Physics (ACAP).

[1] D. Zajfman *et al.*, Phys. Rev. Lett. **75**, 814 (1995).
[2] E. R. Constantinides *et al.*, Geophys. Res. Lett. **6**, 596 (1979).
[3] J. L. Fox, in *Dissociative Recombination: Theory, Experiment and Application*, edited by B. R. Rowe, J. B. A Mitchell, and A. Canosa (Plenum Press, New York, 1993), and references therein.
[4] A. Canosa *et al.*, J. Chem. Phys. **94**, 7159 (1991), and references therein.
[5] S. L. Guberman, Geophys. Res. Lett. **18**, 1051 (1991).
[6] A. Lofthus and P. H. Krupenie, J. Phys. Chem. Ref. Data **6**, 113 (1977).
[7] R. R. Laher and F. R. Gilmore, J. Phys. Chem. Ref. Data **20**, 685 (1991).
[8] S. L. Guberman, in *Dissociative Recombination: Theory, Experiment and Application*, edited by D. Zajfman, J. B. A. Mitchell, D. Schwalm, and B. R. Rowe (World Scientific, Singapore, 1996).
[9] S. P. Möller, in *IEEE Particle Accelerator Conference*, edited by K. Berkner (IEEE, New York, 1991).
[10] K. O. Nielsen, Nucl. Instrum. Methods **1**, 289 (1957).
[11] L. H. Andersen *et al.*, Phys. Rev. A **41**, 1293 (1990).
[12] L. Vejby-Christensen *et al.*, Phys. Rev. A **53**, 2371 (1996).
[13] D. Kella *et al.*, Nucl. Instrum. Methods Phys. Res., Sect. A **329**, 440 (1993).
[14] Z. Amitay *et al.*, Phys. Rev. A **50**, 2304 (1994).
[15] Z. Amitay (private communication).
[16] J. L. Queffelec *et al.*, Planet. Space Sci. **33**, 263 (1985).
[17] S. L. Guberman (private communication).
[18] To convert between the quantum yields and the branching ratios one may use $Y(N(^2D)) = b_a + 2b_c$ and $Y(N(^4S)) = b_a + b_b$. Assuming that N(^2P) converts rapidly to a ^2D atom one can add to the first equation $+b_b$.
[19] K. A. Berrington and P. G. Burke, Planet. Space Sci. **29**, 377 (1981).
[20] A. O. Nier and M. B. McElroy, Science **194**, 1298 (1976).
[21] M. K. Wallis, Planet. Space Sci. **26**, 949 (1978).